

A quantitative analysis of connexin-specific permeability differences of gap junctions expressed in HeLa transfectants and *Xenopus* oocytes

Fengli Cao¹, Reiner Eckert², Claudia Elfgang³, Johannes M. Nitsche⁴, Scott A. Snyder¹, Dieter F. Hülser², Klaus Willecke³ and Bruce J. Nicholson^{1,*}

¹Department of Biological Sciences, State University of New York at Buffalo, Buffalo, NY 14260, USA

²Abt. Biophysik, Biologisches Institut, Universität Stuttgart, Pfaffenwaldring 57, D-70550 Stuttgart, Germany

³Abt. Molekulargenetik, Institut für Genetik, Universität Bonn, Römerstrasse 164, D-53117 Bonn, Germany

⁴Department of Chemical Engineering, State University of New York at Buffalo, Buffalo, NY 14260, USA

*Author for correspondence (e-mail: bjn@acsu.buffalo.edu)

Accepted 8 October 1997; published on WWW 11 December 1997

SUMMARY

Gap junctions provide direct intercellular communication by linking adjacent cells with aqueous pores permeable to molecules up to 1 kDa in molecular mass and 8-14 Å in diameter. The identification of over a dozen connexins in the mammalian gap junction family has stimulated interest in the functional significance of this diversity, including the possibility of selectivity for permeants as seen in other channel classes. Here we present a quantitative comparison of channel permeabilities of different connexins expressed in both HeLa transfectants (rat Cx26, rat Cx32 and mouse Cx45) and *Xenopus* oocytes (rat Cx26 and rat Cx32). In HeLa cells, we examined permeability to two fluorescent molecules: Lucifer Yellow (LY: anionic, MW 457) and 4',6-diamidino-2-phenylindole, dihydrochloride (DAPI, cationic, MW 350). A comparison of the kinetics of fluorescent dye transfer showed Cx32, Cx26 and Cx45 to have progressively decreasing permeabilities to LY, but increasing permeabilities to DAPI. This pattern was

inconsistent with selection based on physical size of the probe, nor could it be accounted for by the differences between clones in the electrical conductance of the monolayers. In *Xenopus* oocytes, where electrical and dye coupling could be assessed in the same cells, Cx32 coupled oocytes showed an estimated 6-fold greater permeability to LY than those coupled by Cx26, a comparable result to that seen in HeLa cells, where an approximately 9-fold difference was seen. The oocyte system also allowed an examination of Cx32/Cx26 heterotypic gap junction that proved to have a permeability intermediate between the two homotypic forms. Thus, independent of the expression system, it appears that connexins show differential permeabilities that cannot be predicted based on size considerations, but must depend on other features of the probe, such as charge.

Key words: Connexin, Lucifer Yellow, Perm-selectivity

INTRODUCTION

Gap junctions are intercellular protein channels formed by 12 subunits of membrane proteins called connexins. Six subunits are contributed by each cell to form hemichannels called connexons, two of which dock via their extracellular loops to form a continuous aqueous passage between cells. To date, gap junctions remain the only known ubiquitous conduits for the direct exchange of ions and metabolites between cells, and in this capacity they have been found throughout the metazoa. Gap junctions have been implicated in the regulation of early development (Guthrie and Gilula, 1989; Paul, 1995), in the maintenance of homeostasis (Sheridan and Atkinson, 1985; Goodenough, 1992), and in the rapid transmission of electrical signals to synchronize cell response in cardiac or neuronal tissue (Barr et al., 1965; Robertson, 1963; Dermietzel and Spray, 1993). Studies also indicate that some gap junctions can serve as tumor

suppressors (Lee et al., 1991; Loewenstein and Rose, 1992; Rose et al., 1993).

The diverse nature of the connexin family has become apparent over the last 10 years with the cloning of more than a dozen members in the mammals alone (Willecke et al., 1991; Paul, 1995), each with its own characteristic properties (e.g. voltage gating parameters; Nicholson et al., 1993). Each tissue expresses its own fingerprint of connexins that can be modulated during different developmental stages or under different physiological conditions (Risek et al., 1992; Sakamoto et al., 1992; Evans et al., 1993; Neveu et al., 1994). This heterogeneity of connexins within a single tissue has raised questions as to their interactions. Indeed, heterotypic coupling between different mammalian connexins expressed in opposed cells has already been extensively characterized in exogenous expression systems (Barrio et al., 1991; Hennemann et al., 1992b; Elfgang et al., 1995; White et al., 1995). Most recently, evidence for heteromeric interactions of different

connexins within a hemichannel have also been reported (Stauffer, 1995; Jiang and Goodenough, 1996), although it has been questioned if these interactions occur in situ (Sosinsky, 1995).

However, inherent to an understanding of how this array of different components influences the physiological functions of gap junctions is the determination of their relative permeabilities. This has generally been thought to be dictated by size alone, although the influence of charge has been reported in several studies (Flagg-Newton et al., 1979; Brink and Dewey, 1980; Veenstra et al., 1994a,b, 1995). The overall size of the channel has been measured by several biophysical approaches to be 1.5 to 2 nm in diameter. (Electron microscopy: Benedetti and Emmelot, 1968; McNutt and Weinstein, 1970; Unwin and Zampighi, 1980. X-ray diffraction: Makowski et al., 1977. Atomic-force microscopy: Revel et al., 1992; Hoh et al., 1993). These estimates are consistent with the observed upper size limit (~1 kDa) on molecules which can traverse the channel (Flagg-Newton et al., 1979; Schwarzmann et al., 1981; Imanaga et al., 1987). In addition to the variety of fluorescent dyes and their variants that have been used to map size exclusion limits, a variety of metabolites and second messengers (cAMP, IP₃, and Ca²⁺: Saez et al., 1989; Kaisai and Peterson, 1994) have also been demonstrated to pass through gap junctions.

Uniform permeability characteristics have typically been associated with gap junctions. However, when differences were seen, the specific connexin(s) expressed were usually not known. The development of exogenous expression systems has allowed connexin properties to be studied in isolation, revealing apparent permeability differences between several types of connexins (Brisette et al., 1994; Steinberg et al., 1994; Traub et al., 1994). In the most extensive comparison to date, Elfgang et al. (1995) examined a variety of tracer molecules varying in size, shape, and charge, and showed variable transfer efficiencies between cells coupled by different connexins. However, quantitative interpretation of these studies was limited by the fact that the differential permeabilities were not directly normalized to the functional expression levels of the different connexin transfectants. Recently, Veenstra et al. (1995) and T. Suchyna et al. (unpublished observations) have compared ionic permeabilities of several connexins, revealing a significant difference in charge preference of different connexins, with a variation in the relative preference for cations over anions ranging from 1:1.06 to 8:1.

In this report, we present a quantitative analysis of the differential permeabilities to larger permeants of three different gap junction channels composed of rat Cx26, rat Cx32 and mouse Cx45. To eliminate system dependent variables, these connexins have been compared in two distinct, well characterized exogenous expression systems that are documented to have minimal endogenous connexin expression (i.e. human HeLa cells and *Xenopus* oocytes). Two oppositely charged fluorescent dyes, Lucifer Yellow (LY) and 4',6-diamidino-2-phenylindole, dihydrochloride (DAPI), were used in assessing permeability in HeLa transfectants. LY was also used in experiments with *Xenopus* oocytes. By using the more rigorous approach of following the kinetics of dye transfer and normalizing to total intercellular junctional conductance, we provide direct evidence that the connexins we have chosen for analysis have consistently differential permeabilities when

expressed in either HeLa transfectants or *Xenopus* oocytes. The data suggest that features other than size, such as charge, contribute to the distinct permeabilities to larger dyes of the three connexins studied, which is consistent with recent observations by Veenstra et al. (1995) and our laboratory (T. Suchyna et al., unpublished observations) on the differential permeabilities of connexins to small anions.

MATERIALS AND METHODS

Northern analysis of endogenous connexin expression in HeLa cells

Poly(A)⁺ RNA (2 µg) from human HeLa cells, isolated with the oligo-dT mRNA kit of Qiagen, was subjected to agarose electrophoresis (1.2% agarose, 2.2 M formamide) and blotted onto Nitran-Plus membranes. The same membranes were used in commercial multiple tissue northern blots (MTN Human I and II, Clontech Labs, Heidelberg, Germany), containing human poly(A)⁺ RNA (2 µg each) of several human tissues that served as control for identification of human connexin transcripts. As probes, radioactively labelled connexin probes were prepared as follows:

rat Cx26 (*HincII/SmaI* cDNA fragment; Zhang and Nicholson, 1989); mouse Cx30.3 (ALW NI/*Bg/II* cDNA fragment; Hennemann et al., 1992a); mouse Cx31.1 (*Bsu36I/BamHI* cDNA fragment; Hennemann et al., 1992a); rat Cx32 (*EcoRI* cDNA fragment; Paul, 1986); mouse Cx37 (*KpnI* fragment of genomic DNA in pBEHpac18; Elfgang et al., 1995); mouse Cx40 (*NarI/AvaII* fragment of genomic DNA in plasmid pBEHpac18; Hennemann et al., 1992b); rat Cx43 (*HindIII/NheI* cDNA fragment; Beyer et al., 1987); mouse Cx45 (*Aval/BgIII* cDNA fragment; Elfgang et al., 1995); rat Cx46 (*EcoRI* cDNA fragment); and mouse Cx50 (*BalI/EcoRV* genomic DNA fragment; White et al., 1992).

Hybridization in 5× SSPE, 10× Denhardt's solution, 50% formamide, 1% SDS, and 100 µg freshly denatured, sheared salmon sperm DNA was followed by two washes in 2× SSC and 0.5% SDS at 50°C for 40 minutes prior to exposure to X-ray film at -70°C.

Preparation of gap junction expressing cells

HeLa transfectants

HeLa transfectants of rat Cx26, rat Cx32, and mouse Cx45 were isolated and characterized by Elfgang et al. (1995) and Mesnil et al. (1995). These cells showed no significant difference in cell shape and size, although some differences in growth rate have been reported (Mesnil et al., 1995). They were cultivated in Dulbecco's modified Eagle's medium (DMEM) supplemented with penicillin (150 µg/ml), streptomycin (100 µg/ml), puromycin (0.5 µg/ml) (all from Sigma Chemical Co., Deisenhofen, Germany) and 10% fetal calf serum (FCS) at pH 7.4 and 37°C in a humidified incubator with 8% CO₂. Cells were routinely subcultured by trypsinization with a change of medium twice a week. Cells were plated at about 40% confluence in 60 mm plastic Petri dishes in the absence of puromycin, approximately 24 hours before the dye coupling experiment. All cells were allowed to grow to 70%-80% confluence at which point they were subjected to either dye injection (both DAPI and LY injections performed in the same dish) or both dye injection and double whole cell patch-clamping. Initial DAPI/LY comparisons were performed on cells maintained in DMEM. However, for the combined LY injection/electrical recording studies requiring longer times outside the incubator, the cells were kept in phosphate-buffered saline (PBS) to improve control over pH and reduce background fluorescence (Brauner et al., 1990). Since early studies showed that coupling levels in DMEM and PBS could differ (C. Elfgang, unpublished observations), all experiments included internal controls for comparison (either DAPI and LY transfer, or LY transfer and electrical

coupling). Furthermore, we detected no significant change in the intercellular coupling level for the 2 hours within which most experiments were conducted.

Xenopus oocytes

Adult female *Xenopus* toads were anesthetized on ice and ovarian lobes containing stage V and VI oocytes were removed and stored at 18°C in Leibovitz-15 medium (L-15, 1:2 dilution) (Gibco Laboratories, Grand Island, NY, USA) buffered with 12.5 mM Hepes, pH 7.6. Three antibiotics (penicillin, streptomycin and gentamycin) were each added to a concentration of 10 µg/ml. To remove the follicle layer, ovarian lobes were dissected into clumps containing approximately 50 oocytes and incubated in Ca²⁺-free OR-2 solution (83 mM NaCl, 2 mM KCl, 1 mM MgCl₂, 5 mM Tris-buffer, pH 7.5) containing 2 mg/ml collagenase (Sigma Chemical Co., St Louis, MO, USA) for 1 hour (Dasckal et al., 1985). Oocytes were then washed with OR-2 and placed back in L-15. After selection of stage VI oocytes, the follicle layer was then stripped manually with forceps.

Defolliculated oocytes were then pressure injected with 40 nl of either 0.2 ng/nl of antisense oligo deoxy-nucleotide to *Xenopus* Cx38 (nucleotides 327-353, numbering begins at the start of translation) alone, or 0.2 ng/nl oligo mixed with 0.3 ng/nl of either rat Cx26 cRNA or 0.3 ng/nl rat Cx32 cRNA, using an electric microinjector (Drummond Scientific Co., Broomall, PA, USA), and micropipettes pulled from glass capillaries (#3-00-203-G/XL, Drummond Scientific Co., Broomall, PA, USA) with a horizontal micropipette puller (Model P-87, Sutter Instrument Co., Novato, CA, USA). Injected oocytes were incubated at 18°C for 24 hours before manual devitelinization and pairing. Cells were incubated in 10 mg/ml soybean agglutinin (Dahl et al., 1987; Levine et al., 1991) for 10 minutes, after which different combinations of 3 oocytes (see Fig. 4) were manipulated into contact with vegetal poles opposed and facing slightly downward (for the purpose of epifluorescence imaging on an inverted microscope) in 35 mm Petri dishes coated with 1-2 mm of 1% agar. These grouped cells were allowed to sit for 24-36 hours at room temperature before whole cell clamping or dye injection.

Microinjection of fluorescent probes, image recording and data analysis

HeLa transfectants

HeLa transfectants in 60 mm Petri dishes grown to 70%-80% confluence were placed on an inverted microscope (IM35, Zeiss, Oberkochen, Germany) for dye injection. Micropipettes for dye injection were pulled from capillary glass (Hilgenberg Glas., Malsfeld, Germany) with a vertical pipette puller (700C, David Kopf Instruments, Tujunga, CA, USA), and back filled with either a 4% (w/v) solution of Lucifer Yellow CH (LY, Molecular Probes Inc., Eugene, OR, USA) dissolved in 1 M LiCl, or 5 mM 4',6-diamidino-2-phenylindole, dihydrochloride (DAPI, Molecular Probes Inc., Eugene, OR, USA) in 0.2 M LiCl. Both dyes were injected iontophoretically into one cell in a monolayer of HeLa transfectants with a current of 20 nA supplied by the iontophoresis unit of a microelectrode amplifier (L/M-1, modification 500 MΩ, List-Electronic, Darmstadt, Germany). LY was injected for 30 seconds and DAPI injected for 1 minute. Micropipettes were withdrawn from the cells immediately after injection stopped to prevent the strong fluorescence of the micropipette interfering with counting. About 10 injections were done in each dish.

The transfer of dye was monitored by a CCD camera and recorded on video tapes from the beginning of injection until about 5 minutes after injection. These video tapes were then played back and frames stopped every 30 seconds after injection. The total number of cells, or the farthest order of cells (i.e. a measure of the number of junctional interfaces traversed) that received dye were recorded at each time point. The fraction of the first order neighboring cells receiving dye was also recorded.

Xenopus oocytes

Oocyte triplets were incubated for 24-36 hours and only those forming intercellular conductances greater than 10 µS (measured by triple whole cell voltage-clamping) were used for experiments. One oocyte in each triplet was pressure injected with 30 nl of 10 mM LY lithium salt in H₂O using the same method used to inject cRNA. In the cases of Cx32/Cx32/Oligo or Cx32/Cx32/Cx26 combinations, a Cx32 cell was injected. In the cases of Cx26/Cx26/Oligo or Cx26/Cx26/Cx32 combinations, a Cx26 cell was injected. Transfer of LY to the neighboring cells was then monitored by a Quantex fluorescent imaging system (Model QX-7, Quantex Inc., Sunnyvale, CA, USA) equipped with an intensified CCD camera linked to a Nikon inverted epifluorescence microscope (Nikon Diaphot, type 108, Nikon Inc., Garden City, NY, USA), using a 4× plan, phase contrast objective. The injected cells were always placed in the upper right corner of the field (see Fig. 4). The CCD and intensifier on the camera gain controller were fixed for all experiments to ensure identical sensitivity. Calibration of the imaging system showed a linear response of fluorescence intensity to the concentration of LY from 0 µM to 7.4 µM, above which the response of the system is saturated. Fluorescent images of LY transfer were acquired at 10 minutes, 20 minutes, 45 minutes, and 90 minutes after dye injection. Each image is an average of 25 frames taken within one second to increase the signal to noise ratio. The images were stored as files on a PC computer in an 8 bit binary, 256 color gray level format. These files were transferred to a Macintosh computer and NIH Image v1.55b5 shareware was employed to analyze the intensity of fluorescence in the recipient cells. We only used data where the fluorescence intensity in the recipient cell did not exceed the saturation point of the imaging system as determined in prior calibration described above. An outline of the area encompassing all fluorescence in the recipient cell was drawn and the intensity of every pixel within this area was integrated by computer. These integrated intensity data were used as a relative measure of the amount of dye in the recipient oocytes.

Measurement of the intercellular conductance

HeLa transfectants

Double whole cell patch-clamping was used to measure the total intercellular conductance between selected cell pairs in the monolayer. The pipette solution consisted of 120 mM KCl, 10 mM EGTA, 10 mM Hepes, pH 7.2, and 2 mM MgCl₂. The micro-pipettes were prepared with a tip diameter around 1.5 µm, and an input resistance around 1 MΩ. Current recording was done using two List EPC-7 patch clamp amplifiers (List Electronic, Darmstadt, Germany). To avoid interference with voltage dependent gating, junctional conductance was determined by applying pulses of 10 mV amplitude to one cell while the neighboring cell was kept at a constant voltage near its resting potential. To avoid subjectivity, cell dishes were randomly moved on the microscope stage and the two cells nearest to the center were patched. About 10 conductance measurements were made from each dish.

Xenopus oocytes

To measure the individual intercellular conductance between each pair of cells in an oocyte triplet, three voltage clamps (two VCC600, Physiologic Instruments Inc., USA; one GeneClamp500, Axon Instruments Inc., Foster City, CA, USA) were used to clamp all three cells at a constant voltage close to the resting potential. A voltage pulse was applied to one of the cells and the junctional currents to the other two cells were measured (as described by Spray et al., 1981, modified for the three cell case). Three sets of data were obtained by pulsing each of the three cells with the same procedure. These data were used to resolve the three individual junctional conductances between every two cells of the triplet. Due to the high conductances obtained, no problems with voltage sensitivity of the connexins were encountered. Clamping electrodes were prepared from capillary glass

(1B150F-4, World Precision Instruments Inc., Sarasota, FL, USA) by a micropipette puller (Model P-87, Sutter Instrument Co., Novato, CA, USA). The input resistance of all electrodes was around 1 M Ω . Conductances were measured before and after each dye transfer experiment, to ensure that no significant changes occurred during the experiment.

RESULTS

Transfected HeLa cells

Connexin expression in parental and transfected HeLa cells

The characterization and isolation of the HeLa transfectants expressing Cx32, Cx26 and Cx45 has been previously described by Butterweck et al. (1994; Cx45) and Elfgang et al. (1995; Cx26 and 32). All transfectants showed punctate surface immunofluorescence at contact surfaces between cells with the appropriate antibodies, although additional staining was also evident in the cytoplasm of these transfectants, a probable consequence of high levels of exogenous expression. The line of HeLa cells used in these studies show minimal levels of endogenous coupling, with no detectable dye coupling (Elfgang et al., 1995) and intercellular conductances 50-fold less than that seen in the transfectants examined here (compare Eckert et al., 1993). In order to perform a wider screen for connexins, at the greatest level of sensitivity, we extended the characterization of the low levels of endogenous connexin expression with northern blot screens of HeLa poly(A)⁺ RNA, with a human multiple tissue northern as a positive control. Weak, specific transcripts were detected for Cx26, 31.1 and 45. No hybridization was detected in the cases of Cx30, 37, 40, 43, 46 or 50.

While no immunofluorescent signal for Cx45 or 26 was detected in untransfected cells (Butterweck et al., 1994; Elfgang et al., 1995), recently, Hülser et al. (1997) have reported that freeze fractured membranes of HeLa wild-type cells exhibited low but significant immunoreactivity, using anti-Cx45 and gold labelled secondary antibodies. Independent electrophysiological analyses by Eckert et al. (1993) revealed a single major class of intercellular channels in the untransfected cells with a conductance of 30pS. This is comparable to the conductance reported for Cx45 channels (Veenstra et al., 1992), and suggests that the Cx45 transcript may be the only one translated into functional protein. Such a conclusion is consistent with the absence of immunofluorescent signals for Cx26 (Elfgang et al., 1995) and the failure of Cx31.1 to form functional channels (Hennemann et al., 1992a).

Differential LY diffusion in Cx32, Cx26 and Cx45 HeLa transfectants

Data for each connexin transfectant was derived from single clones (Cx32-H, Cx26-C, and Cx45-A). Initial analysis of different clones of HeLa cells transfected with these connexins revealed no significant differences in the transfer of LY to first order neighbors between Cx32 and Cx26 clones, although Cx32 transfectants showed a marked reduction compared to Cx26 and Cx45 transfectants in the transfer of the larger cationic dyes, ethidium bromide and propidium iodide (Elfgang et al., 1995). However, quantitative interpretation of

these results was limited, as only steady state transfer to first order neighbors was considered, with no analysis of kinetics or higher order dye spread. In addition, normalization of these results to expression of functional intercellular channels (measured electrophysiologically), was done under different conditions (room temperature in PBS compared to 37°C in DMEM), on different cell aliquots to those tested for dye transfer. We have subsequently found that this can introduce significant variability in the absolute coupling level of the cells.

This was addressed in the current study by measuring the conductance between cells within the same monolayer as that used for dye transfer. By following the kinetics of dye transfer beyond the first order cells, distinct differences in the permeabilities of different connexin transfectants to LY became apparent. Most Cx32 HeLa cells transferred LY to more than 15 cells and frequently reached the third and fourth order neighboring cells within 5 minutes under the described experimental conditions (Fig. 1A). Cx26 cells usually transferred LY to less than 10 cells and mostly reached only the second order neighbors (Fig. 1B). Only about 50% of Cx45 injected cells showed any intercellular transfer of LY, and the transfer was restricted to one or two neighbors (Fig. 1C). This was nonetheless significantly above background, as only 1% of the wild-type HeLa cells showed LY transfer to any neighbors (Elfgang et al., 1995).

To follow the kinetics of LY intercellular diffusion, the total number of cells receiving dye (Fig. 2A) and the maximum number of intercellular interfaces through which dye transfer could be detected (as reflected in the order of neighbors receiving LY, Fig. 2B) were recorded every 30 seconds for 5 minutes. Cases where no dye transfer was seen (6.7% in Cx32, 20.4% in Cx26, and 46.7% in Cx45) were included in the calculation of the average. LY transferred to three times more cells in Cx32 than in Cx26 cells over the 5 minutes period, and it took Cx32 cells about half as much time as Cx26 cells for transfer to the same order of neighbors.

Although a progressive decrease in the ability of Cx32, Cx26, and Cx45 transfectants to pass LY was clearly evident from these data, the extent of the differences varied depending on the specific transfected clone studied (cf. these results and those of Elfgang et al., 1995), likely related to differing connexin expression levels between different clones and under different conditions. Thus, a quantitative comparison of the relative permeabilities of channels composed of different connexins would clearly require knowledge of the relative levels of functional expression of these connexins in the respective transfectants.

Variation of intercellular conductance in HeLa transfectant monolayers

In order to follow the functional expression of connexins in each dye injection experiment, cell pairs within the monolayer were patch-clamped within two hours of dye injection. Since the pattern and density of cell contacts are likely to influence the expression of gap junctions, isolated cell pairs could not be used for these measurements. As a result, the conductances determined are more akin to tissue conductances rather than junctional conductances, and include contributions from alternative current pathways and membrane leak. Modeling of current flow in a finite monolayer of hexagonal cells

(analogous to the dye diffusion model described below) indicates that this could result in a 2- to 2.5-fold overestimate of the actual junctional conductance between cell pairs, a value that is rather insensitive to the size of the monolayer. Furthermore, the cells to be compared are clonally related and of similar shape, size, packing density and confluence. Hence, the monolayer conductance measurements, while not accurate in an absolute sense, are likely to closely reflect the relative levels of junctional conductance between clones. Fig. 3 shows the distribution of conductance for the three HeLa transfectants studied. Cx32 and Cx26 transfectants have essentially identical average conductance, while Cx45 transfectants have an average conductance approximately 30% lower, with a marked predominance of more poorly coupled cells. Although immunocytochemistry could not be used to compare absolute expression levels between transfectants given undefined differences in antibody affinities, this technique did demonstrate minimal differences in the distribution of the three exogenously expressed connexins in the cell (see Results).

To assess whether the lower coupling levels of Cx45 transfectants compared to Cx32 and Cx26 transfectants could account for the reduced transfer of LY, the distribution of conductances (Fig. 3) and the distribution of dye-coupled pairs (as measured by % of first order neighbors that are coupled, Table 1) were compared. In the case of Cx45 transfectants, 16.7% of primary neighbors of the injected cell received dye (Table 1). An examination of the conductance distribution in this transfectant (Fig. 3C) reveals that this same percentage of the cells would have conductances (60 nS, thus defining the minimum conductance needed for detection of dye transfer. The analogous comparison of Cx26 and Cx32 transfectants yields a similar minimal conductance for dye transfer of ~ 70 nS in the case of Cx26, but a much lower value of ~ 30 nS in the case of Cx32. Given that these numbers are not direct measures of junctional conductance, their absolute values carry little significance. The comparison, however, serves to illustrate that even taking into account the variable coupling of the clones studied, it is clear that Cx32 coupled cells can pass LY at much lower levels of coupling than either Cx26 or Cx45 coupled cells.

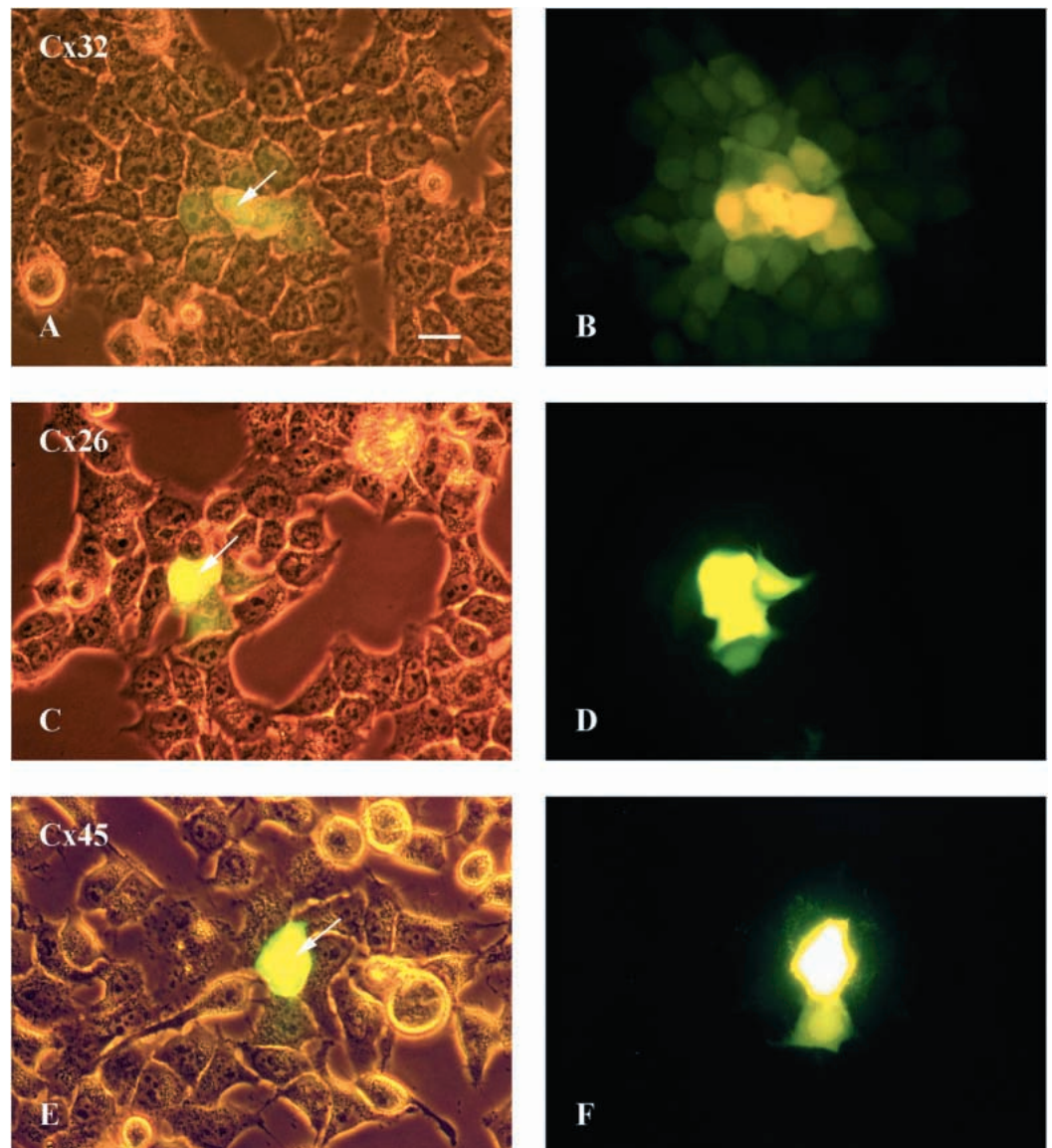


Fig. 1. Fluorescence images showing transfer of LY in HeLa cells transfected with connexins. HeLa transfectants grown to $\sim 80\%$ confluence were injected with 4% (w/v) LY by 30 seconds of iontophoresis and photos were taken 5 minutes after injection. Images of HeLa cells expressing (A,B) Cx32, (C,D) Cx26, and (E,F) Cx45 are shown. Phase contrast images indicating the injected cell (arrow) are shown in A,C,E. Corresponding epifluorescent images of dye transfer are shown in B,D,F. Cx32 transfectant (A,B) has a slightly higher confluence shown here to demonstrate its capability of LY transfer, although in the data shown in Fig. 2 the average confluence of all 3 transfectants was the same. Bar, 10 μm .

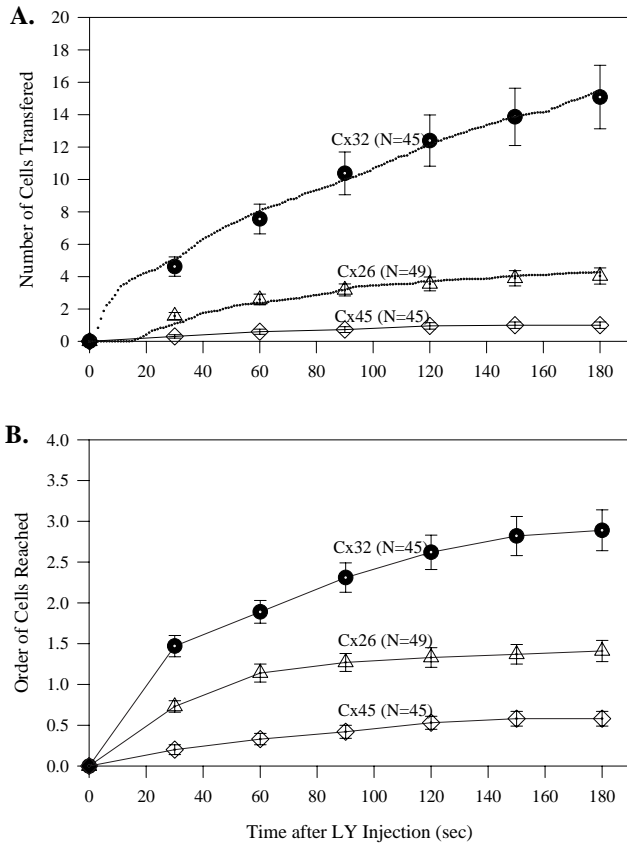


Fig. 2. Quantitative analysis of the kinetics of LY transfer in HeLa transfectants. LY transfer in HeLa cells was recorded on video tape and the number of cells filled with dye at the indicated time points was determined by visual inspection of the appropriate video frames. (A) Average number of the cells surrounding the injected cell that received dye at various time points. (B) The largest order of neighboring cells to receive dye at various times after injection (cells directly adjacent to the injected cells are 1st order neighbors, cells adjacent to 1st order cells are 2nd order neighbors, etc.). N: number of injections being analyzed. (Filled circles) Cx32 clone-H, (open triangles) Cx26 clone-C, (open diamonds) Cx45 clone-A. Dotted curves through the data points for Cx32 and Cx26 in A represent data from 50 iterations of the discrete diffusion model described in the text. Best fits to the data yielded P^j values of 5.34×10^{-6} cm/second for Cx32 and 0.6×10^{-6} cm/second for Cx26.

A quantitative model of dye diffusion in monolayers

To allow a more quantitative comparison of LY transfer between the different HeLa transfectants, we attempted to fit our data to a modification of the model of Ramanan and Brink (1990) that described dye diffusion in a monolayer of cuboidal cells. As a closer approximation to the reality, we represented the HeLa cell monolayer as an array of hexagons, 10 μm in diameter and 2 μm in height. As presented in the original Ramanan and Brink model, net diffusion of dye through the monolayer (D_e) is the sum of its diffusion within the cytoplasm of each cell (D_c), and the permeability of the junctional interfaces between cells (P^j), along with some contributions from transmembrane leak to the medium and irreversible binding to the cytoplasm.

For our purposes we have assumed all of these values, except

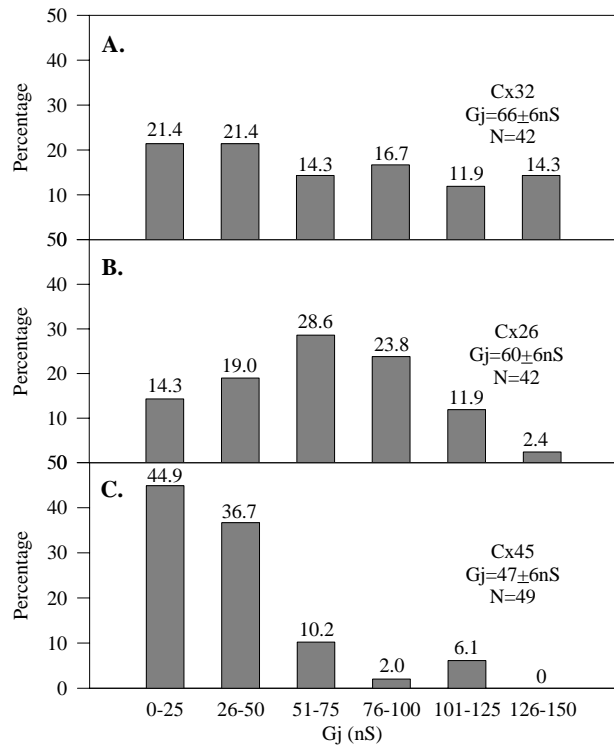


Fig. 3. Distribution of the total intercellular conductances of HeLa transfectants. Conductance was measured by double whole cell patch-clamping of cell pairs in the same dish where dye transfer was assessed (See Fig. 2 and Table 1). Data were collected within 2 hours before or after the dye transfer experiment. HeLa cells expressing (A) Cx32 clone-H, (B) Cx26 clone-C, and (C) Cx45 clone-A are shown. Conductance = mean \pm standard error. N: number of cell pairs recorded.

P^j , to be constant between the different transfectants, since these were clonally derived from the same parent population, and there is no precedent to indicate that connexin expression would modify cytoplasmic properties (or even non-junctional membrane properties in the presence of high extracellular Ca^{2+}). Furthermore, as demonstrated in solutions of the Ramanan and Brink model, the total effective diffusion rate within the monolayer is dominated by the P^j term if the dimensionless parameter $2a \cdot P^j / D_c \leq 1$ (a =average radius of each cell). Reasonable estimates of D_c (1×10^{-7} $\text{cm}^2/\text{second}$; Ramanan and Brink, 1990) and gap junction channel dimensions (1.5 nm diameter, 15 nm length), along with the average measured conductance between cells (Fig. 3), and the known single channel conductances for Cx32 and Cx26 (55 and 135 pS, respectively; Bukauskas et al., 1995; T. Suchyna et al., unpublished observations) lead to an estimation that $2a \cdot P^j / D_c \leq 0.2$. This calculation assumes that the diffusion of dye within the pore is equal to that of bulk cytoplasm. Since LY is likely to encounter significant hindrance in the junctional channel, this is likely to represent an upper estimate of this ratio. Furthermore, the measured values of junctional conductance were obtained from cell pairs in contact with other cells of the monolayer. As noted above, modeling current spread in finite cell populations analogous to that described here for passive dye diffusion indicates that this could increase apparent conductance between cell pairs by up to 2.5-fold (J. M. Nitsche,

unpublished calculations). Thus, the actual $2a \cdot P^j / D_c$ ratio may be smaller still, further justifying the conclusion that junctional permeability is the dominant determinant of dye diffusion within the monolayer.

A limitation to previous models is that some average value of P^j was assigned to all cell-cell interfaces in the population. From the results shown in Figs 1 and 3, the effective coupling of individual cells within the monolayer varies widely, presumably because of differences in expression levels of the transfected connexins. To model this, each cell in the monolayer is randomly assigned an 'expression factor' (f), distributed normally with a mean of 1 and σ of 0.5. P^j from each interface is then calculated as a product of the two expression factors from each cell, and the average $P^j [P^j_{(av)}]$ for the cell population.

In this way, dye flux within any cell m is described as:

$$A \cdot h \cdot \frac{dC_m}{dt} = - \sum_{neighbor\ n} l \cdot h \cdot f_m \cdot f_n \cdot P^j_{(av)} (C_m - C_n),$$

where A =area of cell, h =height of cell (set at 2 μM), l =length of one side of cell ($\sim 5.8 \mu\text{M}$ for a 10 μM diameter hexagon), C_m =concentration of dye in cell m .

For a population of n cells in a monolayer, this yields a system of n coupled differential equations (results are relatively unaffected by the absolute size of the cell population). Initial state is defined as $C_1 = C_{max}$ and $C_2 = C_3 = \dots = C_n = 0$, with cells being scored as receiving dye if C_m exceeds a detection threshold (expressed as a percentage of C_{max}). When an arbitrary $n=37$ was used, the average of 50 solutions to this randomly generated monolayer for both Cx32 and Cx26 transfectants yielded excellent fits to the experimental data (dotted curves in Fig. 2) using a uniform detection threshold for all transfectants of 2%, and best fits (for the $P^j_{(av)}$ of 5.34×10^{-6} cm/second for Cx32 and 0.6×10^{-6} cm/second for Cx26 transfectants. Thus, within the limits of the model presented, the effective permeability of Cx32 junctions for LY is 9-fold that of Cx26. The limited extent of diffusion in Cx45 transfectants prevented adequate modeling of this data.

Comparison of the permeabilities between LY and DAPI

With a clear demonstration that connexin composition can influence the permeability of gap junctions to a larger dye, we

sought to better define what properties of the permeant may influence its permeability. To this end, we undertook a parallel study on a second dye, 4',6-diamidino-2-phenylindole dihydrochloride (DAPI), that is cationic and slightly smaller than LY. DAPI transfers between cells coupled by all connexins we have tested (Cx26, Cx32, and Cx45, Table 1; and Cx37, Cx40, Cx43, data not shown). Because of its tendency to bind DNA, the nucleus of the DAPI injected cell labeled rapidly, as did the nuclei of neighboring coupled cells within 30 seconds to 1 minute of transfer. Labeling was most intense on the side facing the injected cell, and slowly spread to the other side. This pattern provided confirmation that transfer is mediated through gap junctional coupling, rather than by other routes such as leakage to the medium or trapping underneath the cell monolayer.

Because of the binding to nuclear DNA, and its relatively low solubility, DAPI seldom transfers to second order neighbors, and transfer kinetics is slow. For this reason, we only recorded the number of first order neighbors receiving dye 10 minutes after injection. Strikingly, the efficiency of DAPI transfer was the reverse of LY, with the best transfer in Cx26 and Cx45 expressing cells, and significantly less in the Cx32 expressing HeLa clone (Table 1). Although Cx26 and Cx45 transfectants showed relatively similar transfer, normalization to overall conductance would suggest that Cx45 gap junctional channels transfer DAPI with higher efficiency. This limited diffusion of DAPI, as noted above, also precluded application of the quantitative modeling used for the LY studies. However, it is clear that the order of permeabilities is reversed for DAPI compared to LY: Cx45 > Cx26 > Cx32.

Xenopus oocytes

Transfer of LY between Cx32, Cx26 and Cx32/Cx26 coupled oocytes

Although dye transfer is more readily detected in injections of smaller mammalian cells, the *Xenopus* oocyte expression system offers the advantage of direct quantitation of electrical coupling and dye transfer in the same cell pair. *Xenopus* oocytes were injected with antisense oligonucleotide to *Xenopus* Cx38 alone, or mixed with connexin cRNA and then combined in triplets, with vegetal poles opposed (Fig. 4A). This allowed internal controls for background to be incorporated into each measurement in the form of one antisense injected oocyte in each triplet, thus minimizing the effect of variability between oocytes. Electrical conductance between all cells was determined using three independent whole cell voltage clamps. Since the average volume of the oocytes is about 10^6 -fold that of HeLa cells (1 mm in diameter compared to 10 μm), while the average junctional conductance of oocytes is only 10^3 -fold that of HeLa cells (50 μS compared to ~ 50 nS), the accumulation of LY fluorescence in the recipient oocyte is much slower. This required the use of oocyte pairs with higher conductance (10 μS to 50 μS), and a much longer observation time scale (up to 90 minutes). In all cases, no conductance was detected in pairings with oocytes injected with antisense oligo alone. 30 nl LY (10 mM, 0.45%, w/v) was injected into one of the 2 cRNA injected cells (the top right oocyte in Fig. 4) and images were taken at various time points. Experiments on individual oocytes using even lower LY levels showed less than 10% of injected LY bound to the oocyte yolk (data not shown). This, combined with the large excess of LY

Table 1. LY and DAPI transfer in HeLa cells transfected with Cx32, Cx26 or Cx45

Transfectants	% of 1° neighbor†	% of injection cases‡	n§
A. LY (MW* 443, charge -2)			
HeLa-Cx32	71.6	93.3	45
HeLa-Cx26	41.6	79.6	49
HeLa-Cx45	16.7	53.3	45
B. (DAPI: MW* 279, charge +2)			
HeLa-Cx32	26.4	70.7	41
HeLa-Cx26	59.6	93.5	31
HeLa-Cx45	60.0	92.9	14

*Molecular masses of dyes do not include counter ions.

†Percentage of immediate neighbors to the injected cell receiving dye after 10 minutes.

‡Percentage of injections that showed transfer to at least one neighbor.

§Total number of injections.

in the donor cell (see Fig. 4), and restriction of the time frame over which dye transfer is quantitated to 10 minutes (see Fig. 6A), allowed us to treat the donor cell as a constant source of fluorescent probe. Problems of quenching of fluorescence from the pigmented animal pole were avoided by measuring dye spread in the recipient cell only while it remained restricted to the vegetal pole. Consistent with our HeLa cell data, Cx32 gap junctions always showed efficient transfer of LY between

oocytes, at least at conductances above $10 \mu\text{S}$ (Fig. 4B), while Cx26 injected oocytes showed only minimal transfer compared to the negative control (Fig. 4C).

Xenopus oocytes also offered a unique system to study the permeability of heterotypic Cx32/Cx26 gap junctions. Oocyte triplets containing either two Cx32 and one Cx26 injected oocyte (Fig. 4D) or two Cx26 and one Cx32 injected cell (Fig. 4E) were formed. This allowed the transfer of LY across

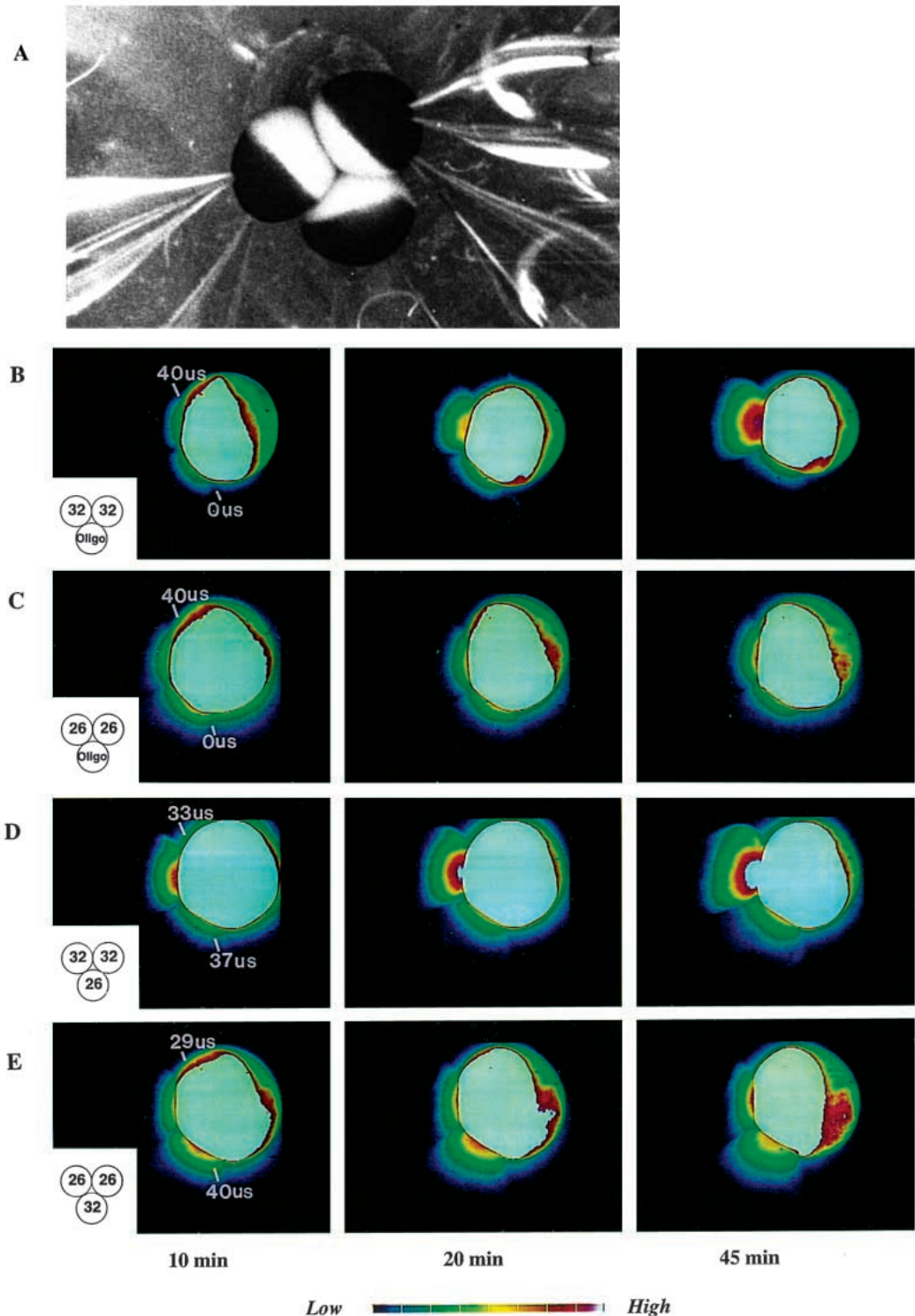


Fig. 4. Time course of LY transfer in *Xenopus* oocytes expressing different connexins. Oocytes were injected with cRNA of the specified connexin and paired in triplets as shown (lower left corner of each image in the first column). Conductance between each pair of cells was determined before and/or after dye injection by clamping all three cells (A), giving a pulse to one cell and measuring the current change in the other two. The cells were then injected with 30 nl of 10 nM LY and images were taken by a Quantex imaging system at indicated time points. The pseudo-color scale used is indicated below the figure. Notice that LY was always injected into the cell on the upper right, and the conductances between the cells of the triplet are as indicated. Transfer of LY across Cx32 homotypic junctions (B) significantly exceeded that across Cx26 homotypic junctions (C). Flux of LY across heterotypic junctions was intermediate between the two homotypic forms, whether the Cx32 (D) or Cx26 (E) cell was injected.

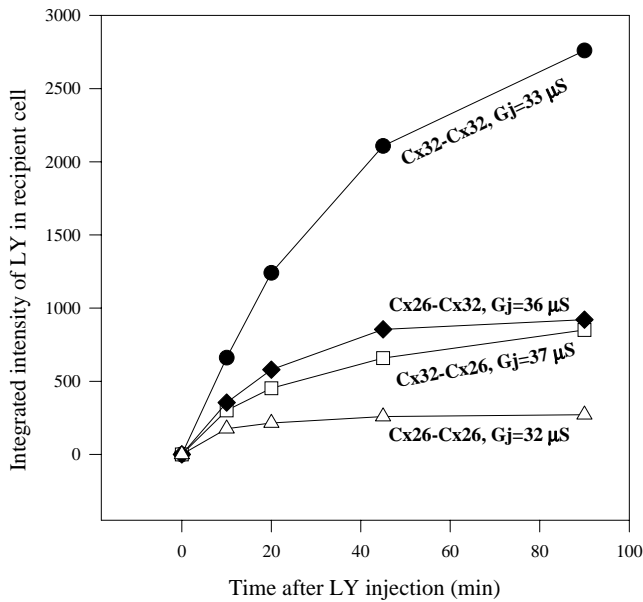


Fig. 5. Quantitation of LY transfer in oocytes from selected triplets with similar conductances. The total fluorescence intensity in the recipient cell was integrated at different times after injection. The numbers shown are arbitrary units given by computer. One example of each type of gap junction is shown. Cx32 (filled circles) and Cx26 (open triangles) homotypic gap junctions, with dye injection into either the Cx26 side (filled diamonds), or the Cx32 side (open squares). Conductance between the cells (G_j) is indicated for each pair.

heterotypic junctions to be normalized within each experiment to that across a homotypic gap junction. Heterotypic junctions displayed a permeability that is intermediate between the two homotypic forms, with little difference in the degree of transfer whether the dye was introduced into the Cx32 (Fig. 4D) or Cx26 (Fig. 4E) expressing cell.

Quantitative measurements of LY permeabilities

For quantitative analysis, dye transfer was measured by integrating the total fluorescence intensity in the recipient cell using a Quantex imaging system. The level of LY injection precluded accurate quantitation of LY in the donor cell, which, as a first approximation, could be considered an 'infinite' source. Fig. 5 shows a time course of dye transfer across gap junctions between oocytes that express different connexins, but develop similar conductances. Electrical conductance between oocytes was also measured after LY transfer, demonstrating that coupling varied by less than 5% over the course of the experiment.

To compare the relative permeabilities of the different gap junction types, we plotted the junctional conductance of each cell pair against the increase of fluorescence intensity in the recipient cell from 10 minutes to 20 minutes (Fig. 6A). Compared to other time points, this is optimal for estimation of junctional permeability with minimal error from transmembrane leakage, binding of dye to yolk, and nonlinear response of the detection system. The slopes (k) of the best fits to the intercellular conductance vs rate of LY transfer plots shown in Fig. 6A provides a direct measure of the relative permeability of

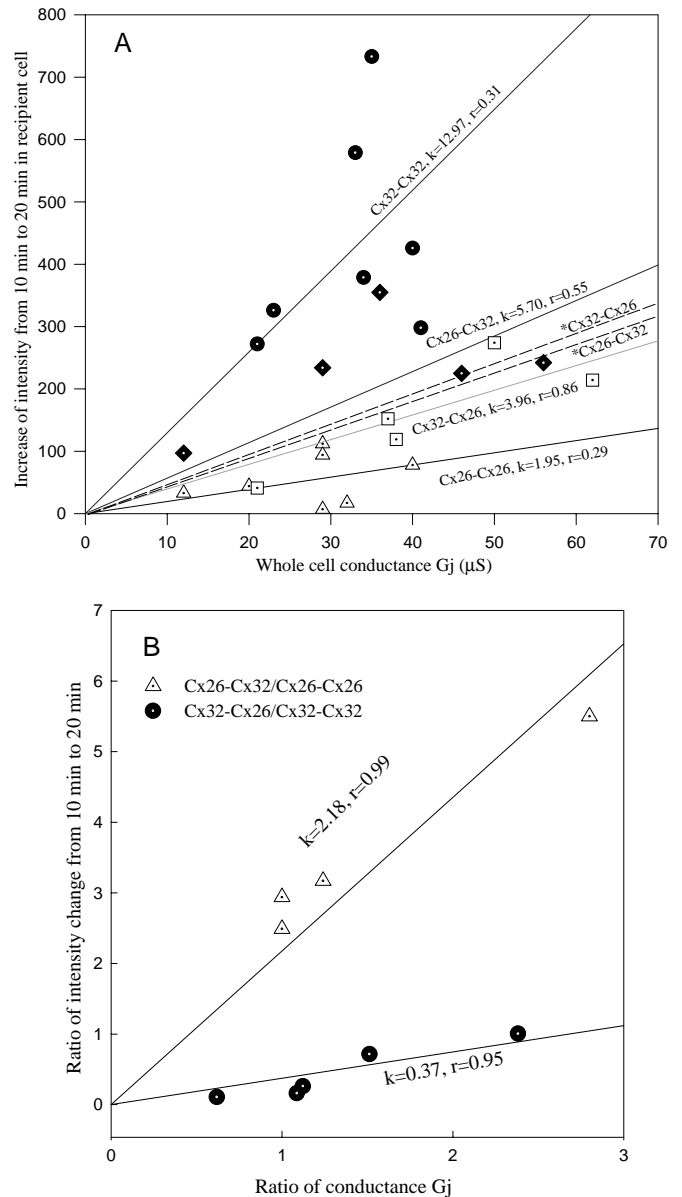


Fig. 6. Analysis of the relative permeabilities of different gap junctions expressed in oocytes. (A) The changes of fluorescence intensity in the recipient cell from 10 minutes to 20 minutes are plotted against conductance for each cell pair. The slope (k) of the best linear fit (r =correlation coefficient) to each set of data provides a direct measure of the LY permeability of Cx32 (filled circles) and Cx26 (open triangles) homotypic junctions and Cx32/Cx26 heterotypic channels, with transfer from either the Cx26 (filled diamonds) or Cx32 cell (open squares). The scatter in the data reflect significant variations between oocyte batches. A correction for this in the case of the heterotypic channels, described in B, produced the dotted curves marked with an asterisk. (B) The ratio of the two sets of dye transfer data that arise from each triplet are plotted against the ratio of the two corresponding G_j s. The slope of the plot indicates the relative permeabilities of the two different forms (i.e. heterotypic and homotypic, as marked). Applying these ratios to the permeability values determined for the homotypic forms (see A) gave very similar permeabilities for the two directions of transfer across heterotypic junctions (dotted lines in A). See text for detailed explanation.

each type of junction. This analysis indicates that Cx32 has approximately sixfold higher permeability to LY than Cx26.

One factor that complicates interpretation of these results is the high conductances that are needed to detect coupling. For conductances over 10 μS , access resistance to the junctions contributes a significant fraction of the voltage drop, leading to systematic underestimation of the actual junctional conductance. While this is difficult to correct formally, an indication that it does not substantially affect the conclusions is provided by restricting comparisons to groups of oocytes with similar conductances (and hence similar errors attributable to access resistance). Our data (Fig. 6A) allowed for such comparisons at 20, 30 and 40 μS ($\pm 10\%$), yielding permeability ratios for LY between Cx32 and Cx26 coupled oocytes of 6, 10 and 5, respectively. These values match closely the 6.5-fold ratio of k values derived from the whole range of conductances (slopes of curves shown in Fig. 6A).

In heterotypic junctions, dye transfer from Cx26 to Cx32 oocytes appeared at first to be slightly greater than in the opposite direction (Cx32 to Cx26 cell-see solid lines in Fig. 6). However, since all data were obtained in triplets, the passage of LY from Cx32 to Cx26 may be affected by the competing effect of the neighboring Cx32 cell which represents a significant sink for the dye. This would not be the case with dye injections into Cx26 cells which pass dye minimally to the homotypic neighbor. To correct for this effect, we plotted the ratio of the two sets of dye transfer data within a given triplet, against the ratio of the two corresponding conductances (Fig. 6B). The slope of this plot provides a ratio of the permeabilities of the two gap junction forms, homotypic and heterotypic, utilizing only internal comparisons within a given triplet. The high level of correlation in this data reflects the elimination of variability between different oocyte pairings, which contributed to the low correlation coefficients (r) seen in Fig. 6A. In this way, we effectively normalize heterotypic coupling to one of the forms of homotypic coupling. This analysis showed heterotypic permeability from Cx32 to Cx26 to be approximately one third (0.37) of Cx32 homotypic permeability, and Cx26 to Cx32 heterotypic permeability to be approximately twice (2.18) Cx26 homotypic permeability. By applying these factors to the permeabilities of the two homotypic channels to LY determined from the conductance-dye diffusion plot of Fig. 6A, the dotted lines were obtained. These 'normalized' plots of permeability for the heterotypic junctions clearly show no significant difference for the two directions of transfer across heterotypic junctions, confirming what would be predicted from first principles of particle flow through asymmetrical pores.

DISCUSSION

In search of a better understanding of the physiological significance of gap junctions, several earlier studies have investigated the permeability of gap junctions to large molecules (Safranyos and Caveney, 1985; Zimmerman and Rose, 1985; Imanaga et al., 1987;), their size exclusion limits (Flagg-Newton et al., 1979; Schwarzmann et al., 1981), and whether natural metabolites and second messengers can pass

through gap junctions (Saez et al., 1989). Although quantitative data were obtained in some of these studies, permeability of the transjunctional probe was not normalized to the levels of gap junction expression, leading to only qualitative comparisons. In addition, information was usually not available on the type of connexin expressed. We present here a rigorous quantitative approach to assessing the permeabilities of three connexins expressed in both transfected HeLa cells and *Xenopus* oocytes, using two fluorescent dyes of different charge, and normalization to the electrical conductance between the cells. This provides clear evidence for differential permeabilities between connexins, that is not dependent on the expression system used and appears to be influenced in part by the charge of the permeant.

On face value, some of our results appear at odds with previously published works. Steinberg et al. (1994) found no LY transfer between cells transfected with chick Cx45. Although limited, we do see LY transfer through HeLa cells expressing mouse Cx45. However, a comparison will reveal that our cells typically show 10-fold higher levels of electrical coupling. Furthermore, initial experiments with Cx43 transfected HeLa cells indicate a dye transfer behavior intermediate between that of Cx45 and Cx32 expressing cells (unpublished observations), consistent with the preferred transfer of LY in Cx43 expressing cells reported by Steinberg et al. (1994). Using different HeLa transfectant clones, Elfgang et al. (1995) found no striking differences in LY transfer between Cx32 and Cx26 expressing cells. The apparent disparity between these earlier results and those presented here in part are likely to reflect different expression levels of connexins in the different clones used in this study, and are in part an artificial product of the way in which data was collected. Steady state dye transfer to 1st order cells can readily saturate and obscure differences in dye transfer that are revealed in kinetics and absolute levels of dye transfer. Hence, while the level of transfer over 3 minutes to 1st order neighbors was comparable between the Cx32 and Cx26 clones, when transfer to higher order cells was considered differences became apparent in both total level of transfer (3rd order cells in Cx32, 2nd order cells in Cx26), and rates of transfer (minutes to fill 1st order cells, with Cx26 and Cx32 transfectants). These numbers showed smaller differences than reported here in Fig. 2 and Table 1. This was likely to reflect differences in expression levels of clones (we used a different Cx32 clone in the current studies). The later was difficult to directly assess, as in the previous study, conductance measurements were performed on different plates of cells tested under different conditions (PBS, 22°C) than the dye injections (DMEM, 37°C). Given the variation in intercellular conductances we have detected between different clones, and even different plates of the same clone (Fig. 3), these comparisons illustrate the necessity of measuring intercellular conductances in the same cell population where dye transfer is measured (as done for the HeLa clones studied here), or, better still, in the same cells (as in the case of oocytes) in order to control for expression levels of the connexins. When this is done, the consistency of the data obtained from very different systems and techniques is remarkable. As illustrated here, various estimates of the relative permeability of Cx32 and Cx26 gap junctions to LY in both mammalian cell monolayers and *Xenopus* oocyte pairs, all yield values between 6-and 9-

fold different when normalized appropriately to total conductance.

It is important to note that the relative permeabilities determined here do not necessarily represent the differential permeabilities at the single channel level, as they have been normalized to the total junctional conductance. Depending on the single channel conductance associated with each connexin, the number of open channels may vary for cells with similar conductance. Even when the single channel conductances are known, the number of open channels may still not be readily evaluated owing to complex issues related to channel density, number in the gap junction plaques and access resistance of the cell (Wilders and Jongsma, 1992). Measurements of conductance in our experiment are used as a method of controlling for the functional expression of gap junctions in terms of the total diffusible aqueous pathway between cells, at least as estimated by the electrically driven diffusion of small ions between cells. Thus, one model that might explain the preferential transfer of LY by Cx32 compared to Cx26 junctions is that, since Cx32 has a smaller single channel conductance than Cx26 (Cx32, 55 pS vs Cx26, 135 pS: Bukauskas et al., 1995; T. Suchyna et al., unpublished observations), Cx32 cells with similar conductance will have 2.5 times more channels than Cx26. If the size of either channel is only big enough to allow one LY molecule to go through at a time, then one would predict that Cx32 cells should show a 2.5-fold better permeability to LY than Cx26 cells with similar intercellular conductance, given the absence of selectivity differences in the channels. This, however, fails to account for the 6 to 9-fold difference in LY permeability measured here, nor the greater permeability to DAPI of Cx26 compared to Cx32 transfected HeLa cells.

What factors contribute to the differential permeability of connexins for fluorescent dyes that have been intimated previously, and are documented here? Size of the probe is likely to be relevant, with DAPI having a significantly narrower profile than LY. However, this cannot account for the reversal in the order of permeabilities to these dyes in the three connexins studied in HeLa cells. Differential interactions of the dyes with the cellular milieu would also affect permeability, but this should be equal for all connexins and again would not explain the reversal in permeabilities of the connexins to the two dyes documented here. The most probable scenario to explain the data presented here is that specific interactions of the dyes with gap junctional channels composed of different connexins influence their permeabilities through the pores. While such interactions may involve shape-dependent binding events that distinguish between the dyes used, the most notable property change between the two fluorescent probes that could account for the different order of permeabilities among connexins is charge. The resulting inference that Cx26 and Cx45 channels show a relative preference for cationic species compared to Cx32 channels (and vice versa for anionic species), is consistent with the reduced rate of ethidium and propidium cation transfer in Cx32 compared to Cx26 and Cx45 transfectants observed previously (Elfgang et al., 1995).

The role of charge selectivity in connexins has already been documented for smaller ionic species through ion substitution studies in N2A transfectants (Veenstra et al., 1995). In

analogous anion substitution experiments done in collaboration with Veenstra, we have demonstrated the same relative cation/anion preference for Cx32 and Cx26 channels as suggested here (T. Suchyna et al., unpublished observations). These analyses provide direct estimates of cation/anion permeability for small ions, and indicate this ratio to be approximately 3 for Cx26 and 1 for Cx32. The lower level of selectivity for ions than larger dyes could be explained in terms of closer electrostatic interactions between the pore and the larger permeants, as well as influence from other structural features that may play a role in modulating permeability.

An intriguing dilemma that arises with the differential permeabilities of junctional channels is the consequences of forming heterotypic gap junctions from hemichannels composed of connexins with different selectivities. In the case of Cx32/Cx26 heterotypic channels, the result is a marked rectification in transjunctional currents with voltages of opposite polarity (Barrio et al., 1991; Bukauskas et al., 1995). However, rectification of these channels should only be revealed on application of a transjunctional potential. By quantitatively assessing the permeability of the Cx32/26 rectifying channels to LY passed in either direction, we have shown that no preferential direction of diffusion was evident in the absence of an applied voltage gradient. However, this behavior remains to be tested in the presence of a constantly applied, or oscillating electrical field, conditions under which electrical rectification would be observed.

The studies presented here, and elsewhere (Veenstra et al., 1995; Elfgang et al., 1995) compel us to no longer view gap junctions as simply aqueous conduits between cells, maintaining homeostasis within a tissue. Rather, they represent a selective filter that preferentially passes certain types of molecules. We have only scratched the surface of the basis of this selectivity, but it appears to be based in part on the charge of the permeant. By extending this quantitative approach to a larger array of permeants, we can begin to map out the specific selectivity features of each connexin. Ultimately, these studies must focus on the biologically significant metabolites, rather than dyes. In this respect, it is important to keep in mind that metabolites which traverse gap junctions are likely to have limited half lives. Thus, unlike other ion channels, rather small changes in relative permeability of the gap junction channels could have significant impact on the transmission of a message between cells. In the current study, we have already documented a 6- to 9-fold variation in the diffusibility of larger permeants through different connexins. Such differences are certain to be critical to understanding the significance of the differential expression of connexins during development, and in response to different physiological conditions, as well as the differential effectiveness of connexins as suppressors of tumor cell growth (Zhu et al., 1992; Bond et al., 1994; Mesnil et al., 1995).

We express our thanks to Beate Rehkopf for preparation of the cells and Jim Stamos for preparation of the figures. This work was supported by NIH grant #HL48773 (B.J.N.), grants Hu204/12-1 (D.F.H.) and SFB284C1 (K.W.) from the Deutsche Forschungsgemeinschaft and Fonds der Chemischen Industrie (K.W.). Bruce Nicholson is an established investigator with the AHA, while Klaus Willecke and Bruce Nicholson share a Max Planck Prize which supported the exchange visit of Fengli Cao to the Willecke lab.

REFERENCES

- Barr, L., Dewey, M. M. and Berger, W. (1965). Propagation of action potentials and the structure of the nexus in cardiac muscle. *J. Gen. Physiol.* **48**, 797-823.
- Barrio, L. C., Suchyna, T., Bargiello, T., Xu, L. X., Roginski, R. S., Bennett, M. V. and Nicholson, B. J. (1991). Gap junctions formed by connexins 26 and 32 alone and in combination are differently affected by applied voltage. *Proc. Nat. Acad. Sci. USA* **88**, 8410-8414.
- Benedetti, E. L. and Emmelot, P. (1968). Hexagonal array of subunits in tight junctions separated from isolated rat liver plasma membranes. *J. Cell Biol.* **38**, 15-24.
- Beyer, E. C., Paul, D. L. and Goodenough, D. A. (1987). Connexin 43: A protein from rat heart homologous to a gap junction protein from liver. *J. Cell Biol.* **105**, 2621-2629.
- Bond, S. L., Bechberger, J. F., Khoo, N. K. and Naus, C. C. (1994). Transfection of C6 glioma cells with connexin 32: the effects of expression of a non-endogenous gap junction protein. *Cell Growth Differ.* **5**, 179-186.
- Brauner, T., Schmid, A. and Hülser, D. F. (1990). Tumor cell invasion and gap junctional communication. I. Normal and malignant cells confronted in monolayer cultures. *Invasion Metast.* **10**, 18-30.
- Brink, P. R. and Dewey, M. M. (1980). Evidence for fixed charge in the nexus. *Nature* **285**, 101-102.
- Brisette, J. L., Kumar, N. M., Gilula, N. B., Hall, J. E. and Dotto, G. P. (1994). Switch in gap junction protein expression is associated with selective changes in junctional permeability during keratinocyte differentiation. *Proc. Nat. Acad. Sci. USA* **91**, 6453-6457.
- Bukauskas, F. F., Elfgang, C., Willecke, K. and Weingart, R. (1995). Heterotypic gap junction channels (connexin 26 or connexin 32) violate the paradigm of unitary conductance. *Pflugers Arch.* **429**, 870-872.
- Butterweck, A., Gergs, U., Elfgang, C. and Willecke, K. (1994). Immunochemical characterization of the gap junction protein connexin 45 in mouse kidney and transfected human HeLa cells. *J. Membr. Biol.* **141**, 247-256.
- Dahl, G., Miller, T., Paul, D., Voellmy, R. and Werner, R. (1987). Expression of functional cell-cell channels from cloned rat liver gap junction complementary DNA. *Science* **236**, 1290-1293.
- Dasckal, N., Gillo, B. and Lass, Y. (1985). Role of calcium mobilization in mediation of acetylcholine-evoked chloride currents in *Xenopus laevis* oocytes. *J. Physiol. (Lond.)* **366**, 299-313.
- Dermietzel, R. and Spray, D. C. (1993). Gap junctions in the brain: where, what type, how many and why? [Review.] *Trends Neurosci.* **16**, 186-192.
- Eckert, R., Dunina-Barkovskaya, A. and Hülser, D. F. (1993). Biophysical characterization of gap-junction channels in HeLa cells. *Pflugers Arch.* **424**, 335-342.
- Elfgang, C., Eckert, R., Lichtenberg-Fratè, H., Butterweck, A., Traub, O., Klein, R. A., Hülser, D. F., Willecke, K. (1995). Specific permeability and selective formation of gap junction channels in connexin-transfected HeLa cells. *J. Cell Biol.* **129**, 805-817.
- Evans, C. W., Eastwood, S., Rains, J., Gruijters, W. T. M., Bullivant, S. and Kistler, J. (1993). Gap junction formation during development of the mouse lens. *Eur. J. Cell Biol.* **60**, 243-249.
- Flagg-Newton, J., Simpson, J. I. and Loewenstein, W. R. (1979). Permeability of the cell-to-cell membrane channels in mammalian cell junction. *Science* **205**, 404-407.
- Goodenough, D. A. (1992). The crystalline lens. A system networked by gap junctional intercellular communication. [Review.] *Semin. Cell Biol.* **3**, 49-58.
- Guthrie, S. C. and Gilula, N. B. (1989). Gap junctional communication and development. *Trends Neurosci.* **12**, 12-16.
- Hennemann, H., Dahl, E., White, J. B., Schwarz, H.-J., Lalley, P. A., Chang, S., Nicholson, B. J. and Willecke, K. (1992a). Two gap junction genes, connexin31.1 and 30.3, are closely linked on mouse chromosome 4 and preferentially expressed in skin. *J. Biol. Chem.* **267**, 17225-17233.
- Hennemann, H., Suchyna, T., Lichtenberg-Fratè, H., Jungbluth, S., Dahl, E., Schwarz, J., Nicholson, B. J. and Willecke, K. (1992b). Molecular cloning and functional expression of mouse connexin 40, a second gap junction gene preferentially expressed in lung. *J. Cell Biol.* **117**, 1299-1310.
- Hoh, J. H., Sosinsky, G. E., Revel, J. P. and Hansma, P. K. (1993). Structure of the extracellular surface of the gap junction by atomic force microscopy. *Biophys. J.* **65**, 149-163.
- Hülser, D. F., Rehkopf, B. and Traub, O. (1997). Dispersed and aggregated gap junction channels identified by immunogold labelling of freeze fractured membranes. *Exp. Cell Res.* **233**, 240-251.
- Imanaga, I., Kameyama, M. and Irisawa, H. (1987). Cell-to-cell diffusion of fluorescent dyes in paired ventricular cells. *Am. J. Physiol.* **252**, H223-H232.
- Jiang, J. X. and Goodenough, D. A. (1996). Heteromeric connexons in lens gap junction channels. *Proc. Nat. Acad. Sci. USA* **93**, 1287-1291.
- Kaisai, H. and Peterson, O. H. (1994). Spatial dynamics of second messengers: IP₃ and cAMP as long-range and associative messengers. *Trends Neurosci.* **17**, 95-101.
- Lee, S. W., Tomasetto, C. and Sager, R. (1991). Positive selection of candidate tumor-suppressor genes by subtractive hybridization. *Proc. Nat. Acad. Sci. USA* **88**, 2825-2829.
- Levine, E., Werner, R. and Dahl, G. (1991). Cell-cell channel formation and lectins. *Am. J. Physiol.* **261**, C1025-C1032.
- Loewenstein, W. R. and Rose, B. (1992). The cell-cell channel in the control of growth. [Review.] *Semin. Cell Biol.* **3**, 59-79.
- Makowski, L., Caspar, D. L. D., Phillips, W. C. and Goodenough, D. A. (1977). Gap junction structures II. Analysis of the x-ray diffraction data. *J. Cell Biol.* **74**, 629-645.
- McNutt, N. S. and Weinstein, R. S. (1970). The ultrastructure of the nexus. A correlated thin-section and freeze-cleave study. *J. Cell Biol.* **47**, 666-688.
- Mesnil, M., Krutovskikh, V., Piccoli, C., Elfgang, C., Traub, O., Willecke, K. and Yamasaki, H. (1995). Negative growth control of HeLa cells by connexin genes-connexin species specificity. *Cancer Res.* **55**, 629-639.
- Neveu, M. J., Sattler, C. A., Sattler, G. L., Hully, J. R., Hertzberg, E. L., Paul, D. L., Nicholson, B. J. and Pitot, M. C. (1994). Differences in the expression of connexin genes in rat hepatomas in vivo and in vitro. *Mol. Carcinogen.* **11**, 145-154.
- Nicholson, B. J., Suchyna, T., Xu, L. X., Hamernick, P., Cao, F., Fourtner, C., Barrio, L. and Bennett, M. V. L. (1993). Divergent properties of different connexins expressed in *Xenopus* oocytes. In *Progress in Cell Research*, vol. 3. (ed. J. E. Hall, G. A. Zampighi and R. M. Davis), pp. 3-13. Elsevier, Amsterdam.
- Paul, D. L. (1986). Molecular cloning of cDNA for rat liver gap junction protein. *J. Cell Biol.* **103**, 123-134.
- Paul, D. L. (1995). New functions for gap junctions. *Curr. Opin. Cell Biol.* **7**, 665-672.
- Ramanan, S. V. and Brink, P. R. (1990). Exact solution of a model of diffusion in an infinite chain or monolayer of cells coupled by gap junctions. *Biophys. J.* **58**, 631-639.
- Revel, J. P., Hoh, J. H., John, S. A., Laird, D. W., Puranam, K. and Yancey, S. B. (1992). Aspects of gap junction structure and assembly. *Semin. Cell Biol.* **3**, 21-28.
- Risek, B., Klier, F. G. and Gilula, N. B. (1992). Multiple gap junction genes are utilized during rat skin and hair development. *Development* **116**, 639-651.
- Robertson, J. D. (1963). The occurrence of a subunit pattern in the unit membranes of club endings in mauthner cell synapses in goldfish brains. *J. Cell Biol.* **19**, 201-221.
- Rose, B., Mehta, P. P. and Loewenstein, W. R. (1993). Gap-junction protein gene suppresses tumorigenicity. *Carcinogenesis* **14**, 1073-1075.
- Saez, J. C., Connor, J. A., Spray, D. C. and Bennett, M. V. (1989). Hepatocyte gap junctions are permeable to the second messenger, inositol 1, 4, 5-trisphosphate, and to calcium ions. *Proc. Nat. Acad. Sci. USA* **86**, 2708-2712.
- Safranyos, R. G. and Caveney, S. (1985). Rates of diffusion of fluorescent molecules via cell-to-cell membrane channels in a developing tissue. *J. Cell Biol.* **100**, 736-747.
- Sakamoto, H., Oyamada, M., Enomoto, K. and Mori, M. (1992). Differential changes in expression of gap junction proteins connexin 26 and 32 during hepatocarcinogenesis in rats. *Jpn J. Cancer Res.* **83**, 1210-1215.
- Schwarzmann, G., Wiegandt, H., Rose, B., Zimmerman, A., Ben-Haim, D. and Loewenstein, W. R. (1981). Diameter of the cell-to-cell junctional membrane channels as probed with neutral molecules. *Science* **213**, 551-553.
- Sheridan, J. D. and Atkinson, M. M. (1985). Physiological roles of permeable junctions: some possibilities. *Annu. Rev. Physiol.* **47**, 337-353.
- Sosinsky, G. (1995). Mixing of connexins in gap junction membrane channels. *Proc. Nat. Acad. Sci. USA* **92**, 9210-9214.
- Spray, D. C., Harris, A. L. and Bennett, M. V. L. (1981). Equilibrium properties of a voltage-dependent junctional conductance. *J. Gen. Physiol.* **77**, 77-93.
- Stauffer, K. A. (1995). The gap junction proteins β_1 -connexin (Cx32) and β_2 -connexin (Cx26) can form heteromeric hemichannels. *J. Biol. Chem.* **270**, 6768-6772.
- Steinberg, T. H., Civitelli, R., Geist, S. T., Robertson, A. J., Hick, E.,

- Veenstra, R. D., Wang, H. Z., Warlow, P. M., Westphale, E. M., Laing, J. G. et al.** (1994). Connexin43 and connexin45 form gap junctions with different molecular permeabilities in osteoblastic cells. *EMBO J.* **13**, 744-750.
- Traub, O., Eckert, R., Lichtenberg-Fratè, H., Elfgang, C., Bastide, B., Scheidtmann, K. H., Hülser, D. F. and Willecke, K.** (1994). Immunochemical and electrophysiological characterization of murine connexin40 and -43 in mouse tissues and transfected human cells. *Eur. J. Cell Biol.* **64**, 101-112.
- Unwin, P. N. and Zampighi, G.** (1980). Structure of the junction between communicating cells. *Nature* **283**, 545-549.
- Veenstra, R. D., Wang, H.-Z., Westphale, E. M. and Beyer, E. C.** (1992). Multiple connexins confer distinct regulatory and conductance properties of gap junctions in developing heart. *Circ. Res.* **71**, 1277-1283.
- Veenstra, R. D., Wang, H. Z., Beyer, E. C. and Brink, P. R.** (1994a). Selective dye and ionic permeability of gap junction channels formed by connexin45. *Circ. Res.* **75**, 483-490.
- Veenstra, R. D., Wang, H. Z., Beyer, E. C., Ramanan, S. V. and Brink, P. R.** (1994b). Connexin 37 forms high conductance gap junction channels with subconductance state activity and selective dye and ionic permeabilities. *Biophys. J.* **66**, 1915-1928.
- Veenstra, R. D., Wang, H. Z., Beblo, D. A., Chilton, M. G., Harris, A. L., Beyer, E. C. and Brink, P. R.** (1995). Selectivity of connexin-specific gap junctions does not correlate with channel conductance. *Circ. Res.* **77**, 1156-1165.
- White, T. W., Bruzzone, R., Goodenough, D. A. and Paul, D. L.** (1992). Mouse Cx50, a functional member of the connexin family of gap junction proteins, is the lens fiber protein MP70. *Mol. Biol. Cell* **3**, 711-720.
- White, T. W., Paul, D. L., Goodenough, D. A. and Bruzzone, R.** (1995). Functional analysis of selective interactions among rodent connexins. *Mol. Biol. Cell* **6**, 459-470.
- Wilders, R. and Jongasma, H. J.** (1992). Limitations of the dual voltage clamp method in assaying conductance and kinetics of gap junction channels. *Biophys. J.* **63**, 942-953.
- Willecke, K., Hennemann, H., Dahl, E., Jungbluth, S. and Heynkes, R.** (1991). The diversity of connexin genes encoding gap junctional proteins. [Review] *Eur. J. Cell Biol.* **56**, 1-7.
- Willecke, K., Heynkes, R., Dahl, E., Stutenkemper, R., Hennemann, H., Jungbluth, S., Suchyna, T. and Nicholson, B. J.** (1991). Mouse connexin37: cloning and functional expression of a gap junction gene highly expressed in lung. *J. Cell Biol.* **114**, 1049-1057.
- Zhang, J.-T. and Nicholson, B. J.** (1989). Sequence and tissue distribution of a second protein of hepatic gap junctions, Cx26, as deduced from its cDNA. *J. Cell Biol.* **109**, 3391-3401.
- Zhu, D., Kidder, G. M., Caveney, S. and Naus, C. C. G.** (1992). Growth retardation in glioma cells cultured with cells over expressing a gap junction protein. *Proc. Nat. Acad. Sci. USA* **89**, 10218-10221.
- Zimmerman, A. L. and Rose, B.** (1985). Permeability properties of cell-to-cell channels: kinetics of fluorescent tracer diffusion through a cell junction. *J. Membr. Biol.* **84**, 269-283.